

27  
25/79  
JULY 15  
24 1979

MASTER

UCID- 18208

# Lawrence Livermore Laboratory

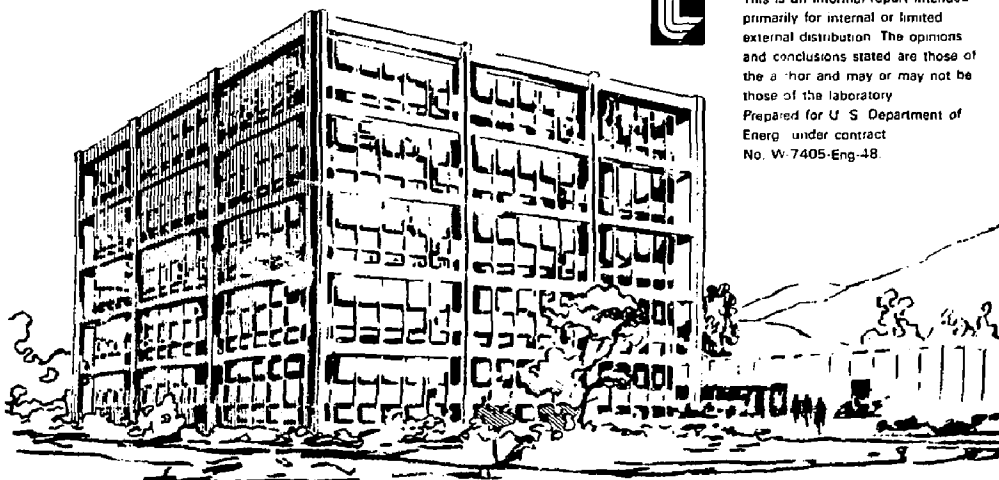
PRELIMINARY REPORT: QATTARA PROJECT MATERIAL PROPERTIES

MARC COSTANTINO

JUNE 1979



This is an informal report intended primarily for internal or limited external distribution. The opinions and conclusions stated are those of the author and may or may not be those of the laboratory.  
Prepared for U S Department of Energy under contract No. W-7405-Eng-48.



*Interdepartmental letterhead*

Mail Station L 350

Ex 26923

20 June 1979

M E M O R A N D U M

TO: John Toman  
FROM: Marc Costantino  
SUBJECT: PRELIMINARY REPORT: QATTARA PROJECT MATERIAL PROPERTIES

We have measured strength under triaxial loading and compressibility under hydrostatic loading for four representative materials along a proposed route of a canal from the Mediterranean Sea to the Qattara Depression. The results of these measurements are used in computer calculations for cratering profiles using nuclear explosives. Considerations of the lithology along the route have led to a characterization of earth material types using four descriptors: 1) limestone, 2) sandstone, 3) high sand, and 4) clay/silt. This memo is a preliminary report of the work and data reduction. A more complete account will be published at a later date.

The organization of this memo is:

- A. Introduction
- B. General description of the as-received cores
- C. Apparatus
- D. Results for limestone
- E. Results for sandstone
- F. Results for high sand
- G. Results for clay/silt

A. Introduction

In August 1978, LLL agreed to undertake calculations of cratering profiles as part of a feasibility study for the Qattara Project. The concept is to use a series of underground nuclear explosions to create a canal between the Mediterranean Sea and the lip of the Qattara Depression in Egypt, a distance of about 80 km. The 60m drop to the Depression floor then provides a hydrostatic head for generating electricity.

In order to perform the cratering calculations, the lithography along the proposed canal route was characterized by dividing it into four broad

**NOTICE**  
This report was prepared at an account funded by the U.S. Government. Neither the United States nor the United States Department of Energy, nor any of their employees, nor any of their contractors, subcontractors, or employees, makes any express or implied assumptions as to the legal status of any material, device, or procedure. It is the responsibility of the user of this report to determine its legal status and to use it in accordance with all applicable laws and regulations. The user is responsible for any damages resulting from its use.



University of California

LAWRENCE LIVERMORE LABORATORY

John Toman  
20 June 1979  
Page 2

geologic types. The actual lithology of the region near an explosion is modeled using one or more of these types, and a computer code is used to predict the crater profile for a particular explosive configuration. Material density, water content, gas-filled porosity, compressibility and strength are required in performing the calculations. The Geophysics Section of the Earth Sciences Division was tasked to make laboratory measurements of compressibility and strength.

B. General Description of the As-Received Cores

On the basis of logs for drill holes C-2, N-1, N-2, N-3, and NN-4, the lithology was modeled as shown in Fig. 1. Samples of core totalling 20m in length (x's in Fig. 1) were requested in September 1978 to be sent to LLL. In December 1978 core samples ranging from 7.5 to 15 cm in diameter and totalling 18.5m in length were delivered (0's in Fig. 1).

In order to decrease the uncertainty of the measurements, the cores were to be preserved as nearly as possible in the in situ condition. Although the intact core samples were wrapped in cotton cloth and adequately waxed, all were quite dry with no evident moisture even for those from below the water table. The clay/silt cores showed through-going cracks, evidently owing to shrinkage, parallel to the bedding and radial cracks along the cylinder axis. The subsequent requirement to reconstitute samples results in increased uncertainty in relating laboratory data to in situ conditions.

C. Apparatus

Four major apparatus were used in this program. Failure curve (strength) measurements on the limestone and sandstone were done in the Washington press, in which  $\sigma_1$  the axial (and major principal) stress and  $\sigma_2 = \sigma_3$  (intermediate and minor principal stresses -- the confining pressure) could be controlled and measured independently and the axial strain measured. Compressibility tests for the limestone and sandstone were made with a purely hydrostatic pressure less than 20MPa using the SOB apparatus and for a quasi-hydrostatic pressure to 3500MPa using the Kennedy press. In the former, strain gauges attached to the copper jacketed samples are used to measure radial and longitudinal strains. In the latter, the volume of the sample inside a deformable tin cup is determined by comparison of axial displacements against a standard material (nickel).

Failure curves for the high sand and clay/silt were determined using for the first time a new apparatus, SASS. SASS permits independent measurements of axial stress ( $\sigma_1$ ) confining pressure ( $\sigma_2 = \sigma_3$ ), radial strain, and longitudinal strain for samples up to 11.5cm in diameter and 18cm long. This apparatus was assembled, tested, and calibrated during the course of the Qattara work. Additionally, sample preparation and jacketing techniques were developed.

D. Limestone

A limestone cap, decreasing in thickness from north to south, covers a portion of the route. Cores from hole C-2 (~19m), termed "chalky" limestone and from N-1 (~47m), termed "fossiliferous" limestone, were tested. Strength curves and hydrostats are shown in Figs. 2 - 5 and the results listed in Tables I and II. All measurements were made for 0% water saturation. At 0.1 MPa confining pressure failure is brittle. However, at 20 and 100 MPa confining pressure the material hardens after yielding at the end of an elastic region. Definitions of the terms used in Figures 3 and 5 are given in Figure 3A.

E. Sandstone

Sandstone samples taken from hole N-3 (~133m) were competent, but friable, with widely scattered inclusions ranging from 1-10mm in diameter. Compressibility for the 100% and 0% saturated sandstone are shown in Fig. 6. Failure curves for 50% and 100% saturations are shown in Figs. 7 and 8. The data are in Tables III and IV. In the case of the partially saturated material, the matrix fails before the pore fluid fills the porosity. The pore fluid pressure then increases upon further compaction and the assemblage of unbonded sand grains has a strength similar to that of high sand. The pore pressure in the fully saturated sandstone increases sufficiently fast to prevent the early matrix collapse and the failure curve shows a normal behavior.

F. High Sand

Since the as-received cores showed significant water loss, the high sand samples were reconstituted by drying in vacuum at 105°C, adding an appropriate amount of water, and compacting to bring the density and water content near to that shown by the well log for hole NN-4 at 310m depth. A sample was made of a stack of five disks, each about 3cm thick and 7cm diameter, using material from the 27m depth of hole NN-4. Since the sample is fully saturated only at and above the overburden pressure, the 0.1 MPa failure point is for less than 100% saturation. The compressibility curve is shown in Fig. 9 and the failure curve in Fig. 10. Data are given in Table V.

G. Clay/Silt

The as-received samples of clay/silt were reconstituted as for the high-sand. Compressibility is shown in Fig. 11 and strength in Fig. 12. Data for the failure curve are in Table VI.

MC:jfc

Attachments

Tables I - VII  
Figures 1 - 12

TABLE I  
 STRENGTH DATA FOR QATTARA CHALKY LIMESTONE  
 UNDER TRIAXIAL LOADING  
 0% SATURATION

	$\tau$ (MPa)	$\bar{\sigma}$ (MPa)
"Elastic" yield	9.5 $\pm$ 1.6 11.8 $\pm$ 3.7 2.5 $\pm$ 0.8	6.4 $\pm$ 1.1 27.9 $\pm$ 2.5 101.7 $\pm$ 0.6
3% Plastic strain	9.5 $\pm$ 1.6 18.7 $\pm$ 0.2 33.6 $\pm$ 11.2	6.4 $\pm$ 1.1 32.4 $\pm$ 0.1 122.4 $\pm$ 7.5
5% Plastic strain	9.5 $\pm$ 1.6 20.2 $\pm$ 0.2 51.2 $\pm$ 10.2	6.4 $\pm$ 1.1 33.4 $\pm$ 0.1 134.0 $\pm$ 7.0
10% Plastic strain	9.5 $\pm$ 1.6 23.2 $\pm$ 0.6 114.8 $\pm$ 30.8	6.4 $\pm$ 1.1 35.4 $\pm$ 0.4 176.4 $\pm$ 20.6

Grain density = 2.84 gm/cm<sup>3</sup>  
 Bulk density = 1.42 gm/cm<sup>3</sup> (0% saturation)  
 Porosity = 0.50

TABLE II  
 STRENGTH DATA FOR QATTARA FOSSILIFEROUS LIMESTONE  
 UNDER TRIAXIAL LOADING  
 0% SATURATION

	$\tau$ (MPa)	$\bar{\sigma}$ (MPa)
"Elastic" yield	6.0 $\pm$ 0.4 3.0 $\pm$ 1.4 3.0 $\pm$ 0.3	4.1 $\pm$ 0.2 22.0 $\pm$ 1.0 102.0 $\pm$ 0.2
3% Plastic strain	6.0 $\pm$ 0.4 11.7 $\pm$ 2.1 44.9 $\pm$ 11.9	4.1 $\pm$ 0.2 27.8 $\pm$ 1.4 129.9 $\pm$ 7.9
5% Plastic strain	6.0 $\pm$ 0.4 12.4 $\pm$ 3.2 66.0 $\pm$ 17.4	4.1 $\pm$ 0.2 29.6 $\pm$ 1.2 144.0 $\pm$ 11.6
10% Plastic strain	6.0 $\pm$ 0.4 20.3 $\pm$ 1.4	4.1 $\pm$ 0.2 33.5 $\pm$ 0.9

Grain density = 2.69 gm/cm<sup>3</sup>

Bulk density = 1.80 gm/cm<sup>3</sup> (0% saturation)

Porosity = 0.33

TABLE III  
 FAILURE STRESS DATA FOR QATTARA SANDSTONE  
 UNDER TRIAXIAL LOADING CONDITIONS  
 ~50% SATURATION

Sample	$\sigma_c$ (MPa)	$\tau_f$ (MPa)	$\bar{\sigma}_f$ (MPa)
Q399	0.1	5.87	4.02
Q390A	0.1	3.24	2.26
Q391A	0.1	6.33	4.32
Q399A	0.1	9.52	6.45
Q393A	20.0	18.44	32.29
Q394A	20.0	7.17	24.78
Q395A	20.0	9.42	26.28
Q398A	20.0	9.52	26.69
Q395A	100.0	4.75	103.2
Q396A	100.0	3.69	102.5
Q397A	100.0	4.22	102.8

AVERAGE VALUES

$\tau_f$ (MPa)	$\bar{\sigma}_f$ (MPa)
$6.2 \pm 2.6$	$4.26 \pm 1.7$
$11.3 \pm 4.9$	$27.51 \pm 3.3$
$4.22 \pm 0.53$	$102.8 \pm 0.4$

Grain density =  $2.77 \text{ gm/cm}^3$   
 Bulk density =  $2.23 \text{ gm/cm}^3$  (0% saturation)  
 Porosity = - 0.19

TABLE IV  
 FAILURE STRESS DATA FOR QATTARA SANDSTONE  
 UNDER TRIAXIAL LOADING CONDITIONS  
 100% SATURATION

Sample	$\sigma_c$ (MPa)	$\tau_f$ (MPa)	$\bar{\sigma}_f$ (MPa)
Q390	0.1	6.03	4.12
Q391	0.1	4.05	2.80
Q392	0.1	9.52	6.45
Q393	20.0	13.86	29.24
Q394	20.0	13.86	29.24
Q395	20.0	5.85	23.90
Q396	100.0	19.62	113.1
Q397	100.0	17.72	111.8
Q398	100.0	15.61	110.4

AVERAGE VALUES

$\tau_f$ (MPa)	$\bar{\sigma}_f$ (MPa)
$6.5 \pm 2.8$	$4.5 \pm 1.8$
$11.2 \pm 4.6$	$27.5 \pm 3.1$
$17.6 \pm 2.0$	$111.8 \pm 1.3$

Grain density =  $2.77 \text{ gm/cm}^3$   
 Bulk density =  $2.23 \text{ gm/cm}^3$  (0% saturation)  
 Porosity = 0.19

TABLE V  
 FAILURE STRESS DATA FOR QATTARA HIGH SAND  
 UNDER TRIAXIAL LOADING CONDITIONS  
 100% SATURATION

Sample	$\sigma_c$ (MPa)	$\tau_f$ (MPa)	$\bar{\sigma}_f$ (MPa)
Q401	0.1	0.17	0.21
Q404	0.1	0.25	0.27
Q407	0.1	0.31	0.31
Q402	20.0	6.3	24.2
Q405	20.0	4.4	22.9
Q408	20.0	4.2	22.8
Q403	100.0	6.5	104.3
Q406	100.0	5.7	103.8
Q409	100.0	5.3	103.5

AVERAGE VALUES

$\tau_f$ (MPa)	$\bar{\sigma}_f$ (MPa)
$0.24 \pm 0.07$	$0.26 \pm .05$
$5.0 \pm 1.2$	$23.3 \pm 0.8$
$5.8 \pm 0.6$	$103.9 \pm 0.4$

Grain density =  $2.70 \text{ gm/cm}^3$

Bulk density =  $2.23 \text{ gm/cm}^3$  (approximately 100% saturation)

Porosity = 0.26

TABLE VI  
 FAILURE STRESS DATA FOR QATTARA CLAY/SILT  
 UNDER TRIAXIAL LOADING CONDITIONS  
 100% SATURATION

Sample	$\sigma_c$ (MPa)	$\tau_f$ (MPa)	$\bar{\sigma}_f$ (MPa)
Q175	0.1	0.28	0.29
Q176	0.1	0.40	0.37
Q179	0.1	0.40	0.37
Q171	20.0	0.71	20.47
Q174	20.0	0.42	20.28
Q177	20.0	0.49	20.33
Q180	20.0	0.55	20.37
Q172	100.0	0.70	100.47
Q178	100.0	0.69	100.46
Q181	100.0	0.68	100.45

AVERAGE VALUES

$\tau_f$ (MPa)	$\bar{\sigma}_f$ (MPa)
$0.4 \pm 0.1$	$0.3 \pm 0.1$
$0.5 \pm 0.1$	$20.4 \pm 0.1$
$0.7 \pm 0.01$	$100.5 \pm 0.01$

Grain density =  $2.85 \text{ gm/cm}^3$

Bulk density =  $2.06 \text{ gm/cm}^3$  (approximately 100% saturation)

TABLE VII  
BRAZIL TEST RESULTS FOR QATTARA LIMESTONE  
0% SATURATION

A. CHALKY LIMESTONE

Sample	$\tau_f$ (MPa)
Q378	3.8
Q379	2.0
Q370A	3.3
Q371A	3.0
Q372A	6.3
Q373A	2.4

$\tau_f$  (Avg.) =  $3.5 \pm 1.5$

B. FOSSILIFEROUS LIMESTONE

Sample	$\tau_f$ (MPa)
Q228	4.2
Q229	2.7
Q220	3.7
Q221A	2.9
Q222A	2.2
Q223A	2.8
Q224A	2.5

$\tau_f$  (Avg.) =  $3.0 \pm 0.7$

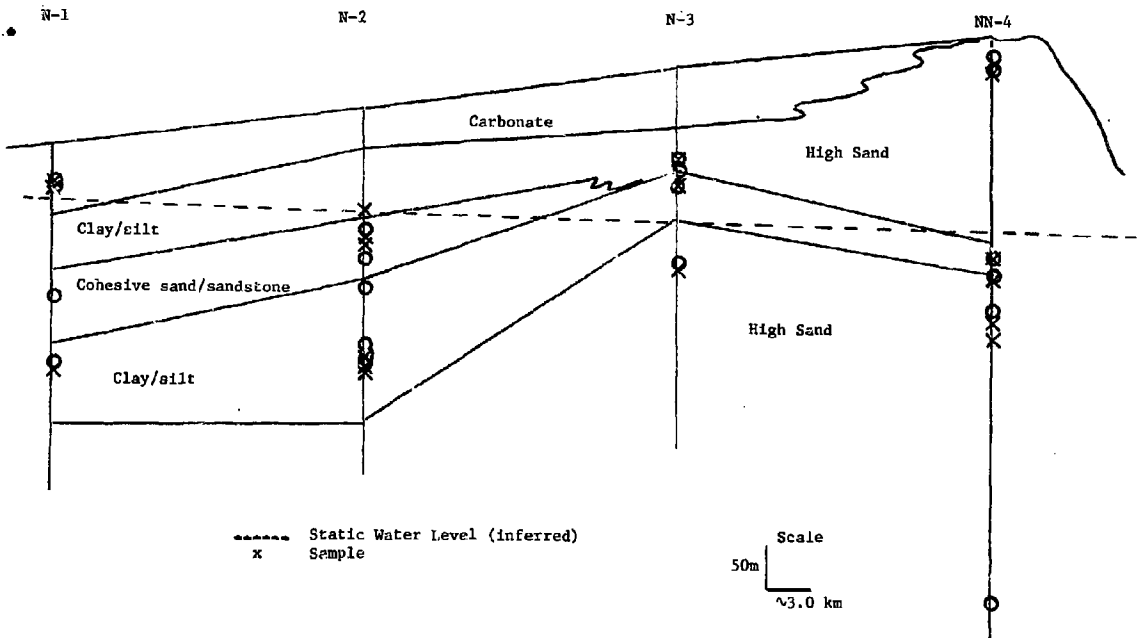


FIGURE 1  
MODEL LITHOGRAPHY

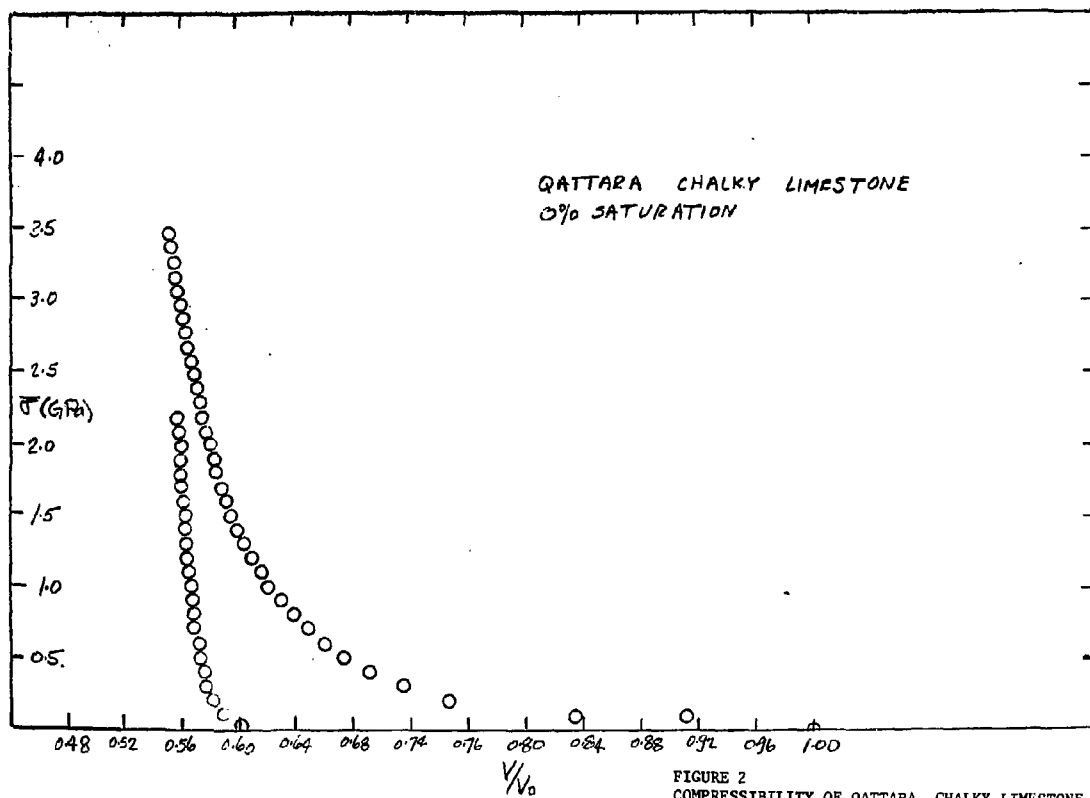


FIGURE 2  
COMPRESSIBILITY OF QATTARA CHALKY LIMESTONE

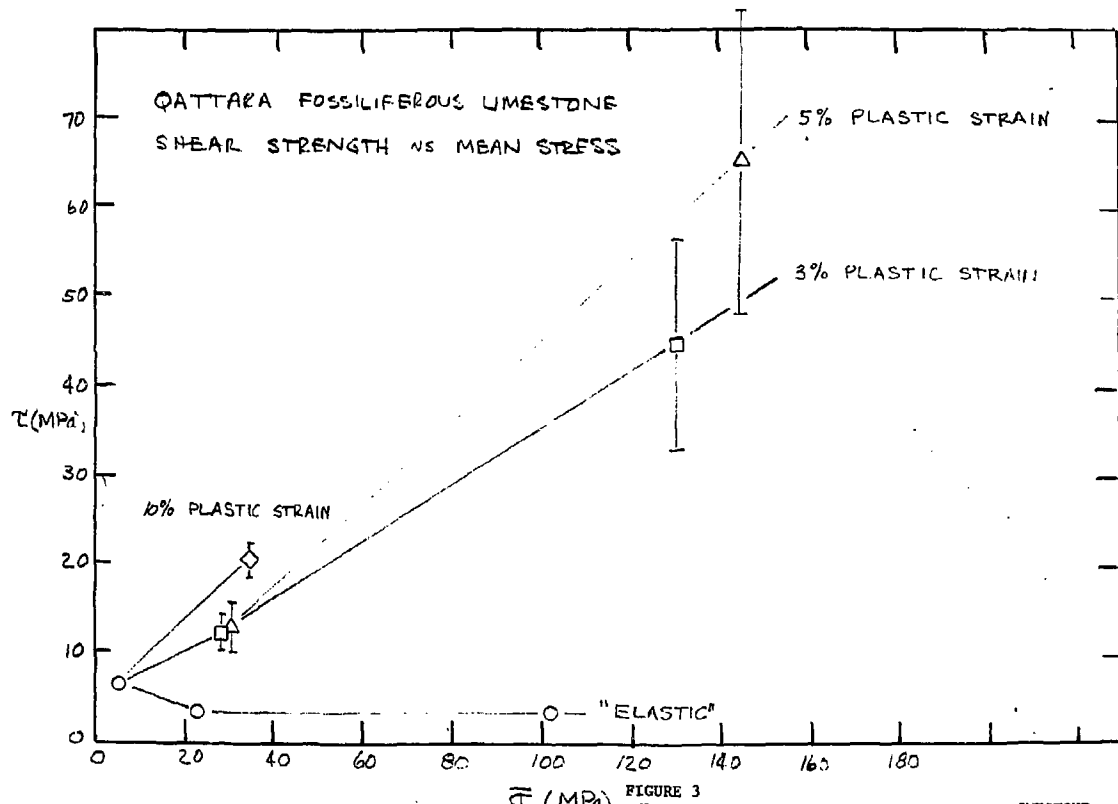
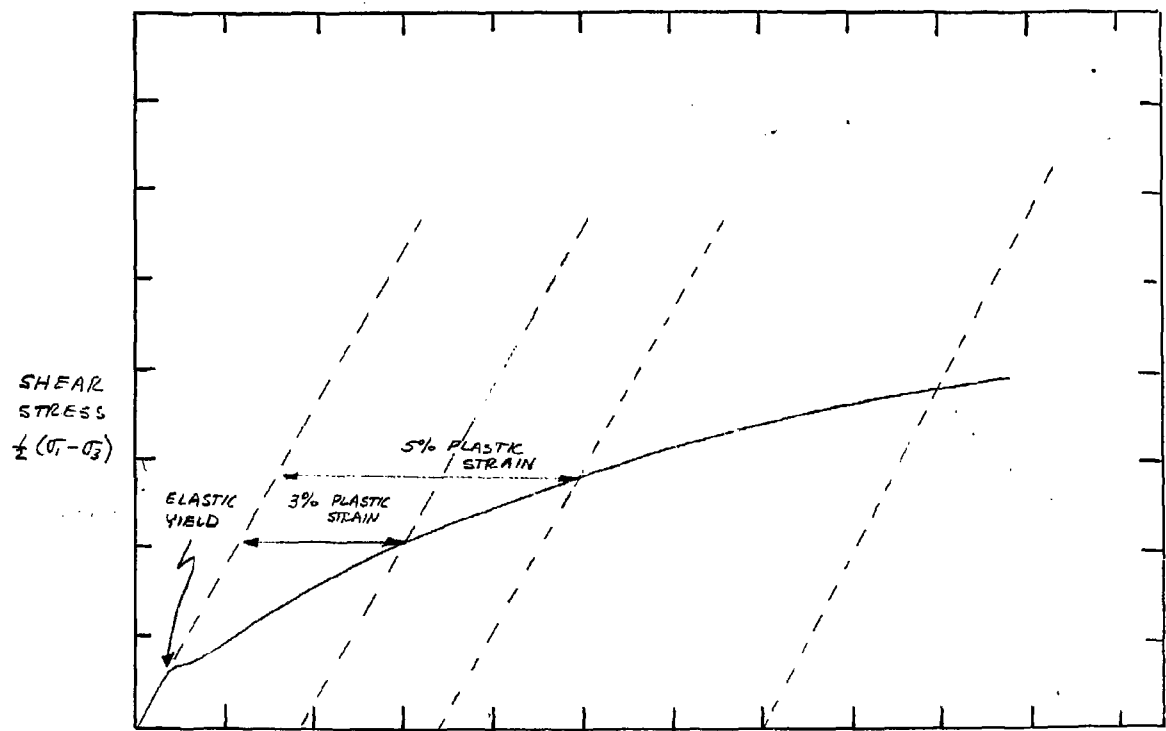


FIGURE 3  
STRENGTH CURVE FOR QATTARA FOSSILIFEROUS LIMESTONE



AXIAL DISPLACEMENT  
(ARBITRARY UNITS)

FIGURE 3A

SCHEMATIC OF LOADING CURVE FOR QATTARA LIMESTONE

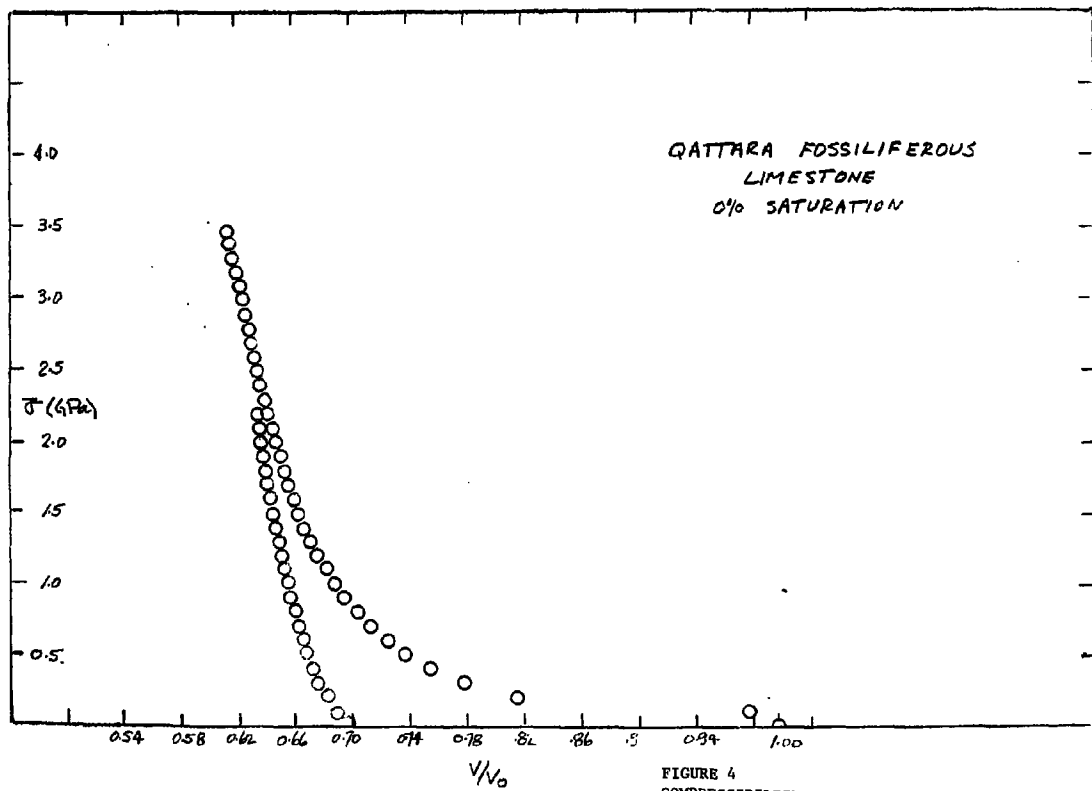
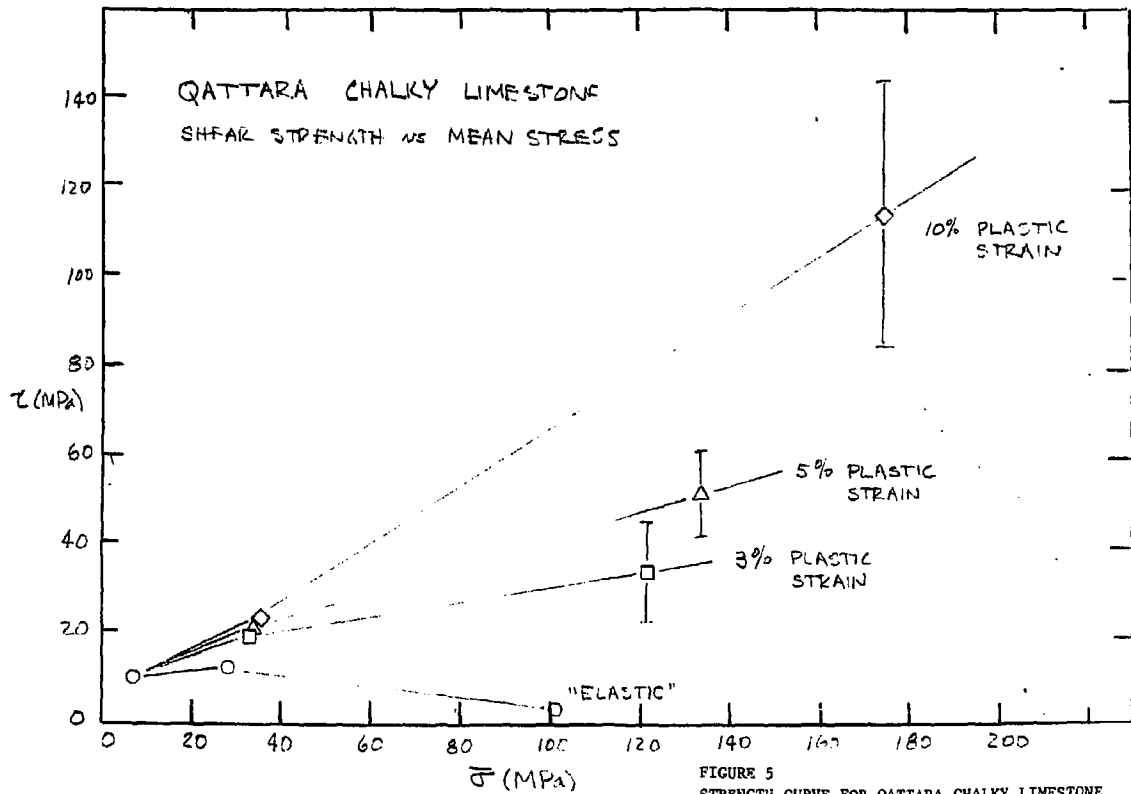


FIGURE 4  
COMPRESSIBILITY OF QATTARA FOSSILIFEROUS LIMESTONE



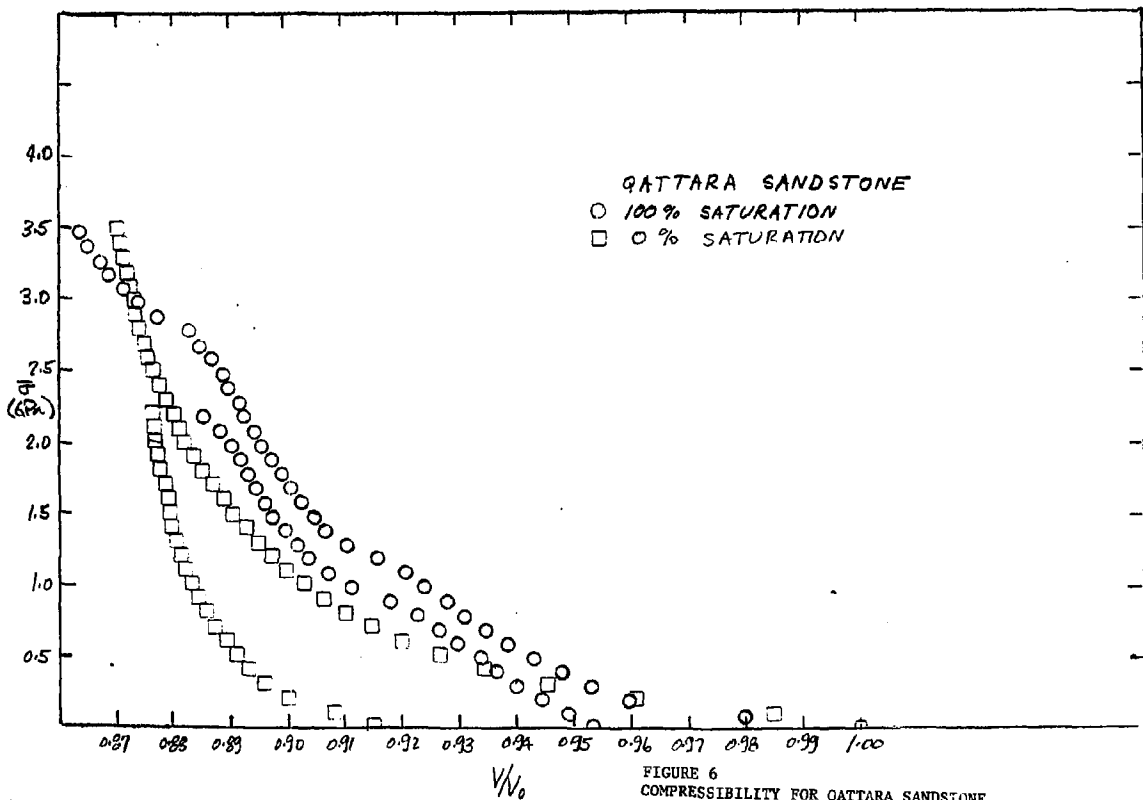


FIGURE 6  
COMPRESSIBILITY FOR QATTARA SANDSTONE

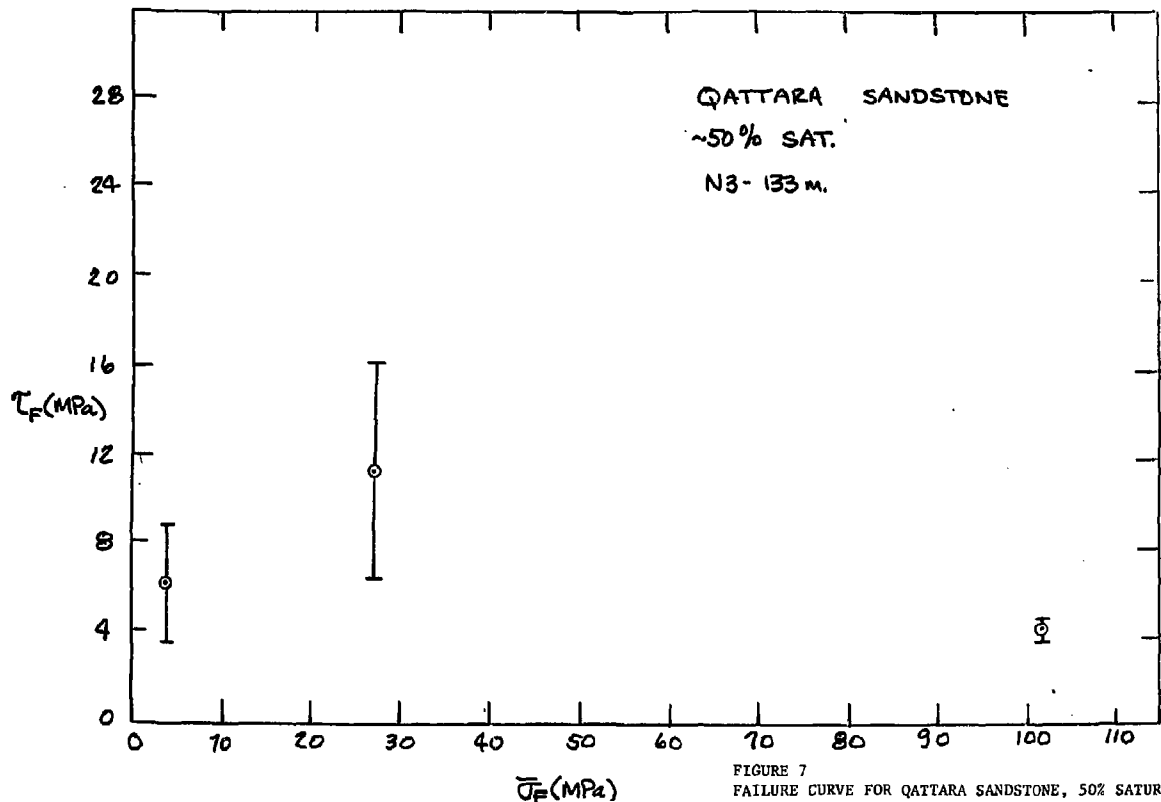


FIGURE 7  
FAILURE CURVE FOR QATTARA SANDSTONE, 50% SATURAT.

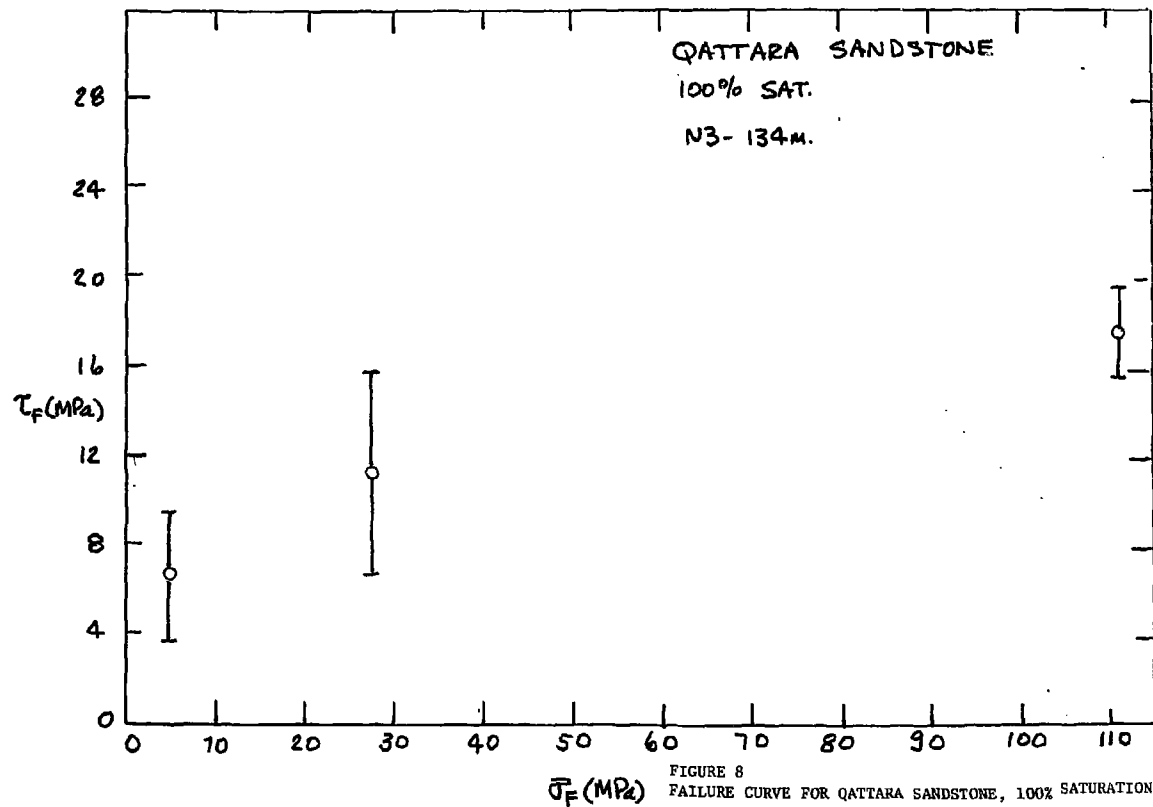


FIGURE 8  
FAILURE CURVE FOR QATTARA SANDSTONE, 100% SATURATION

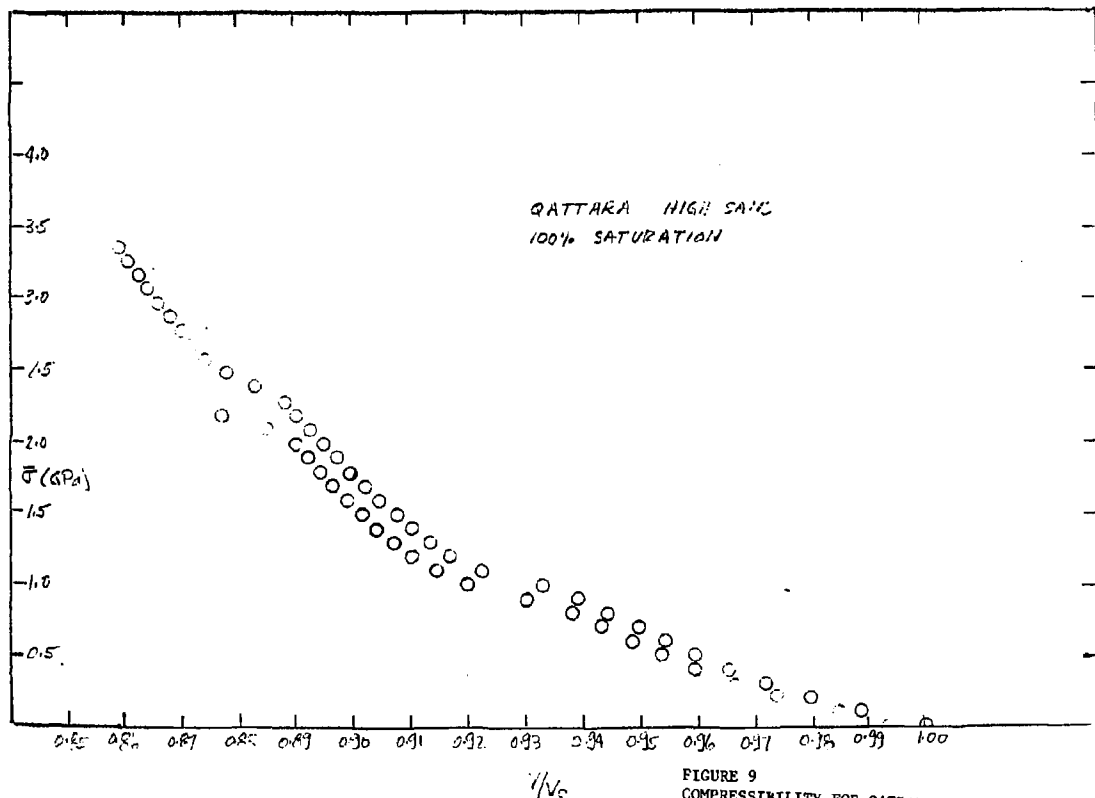
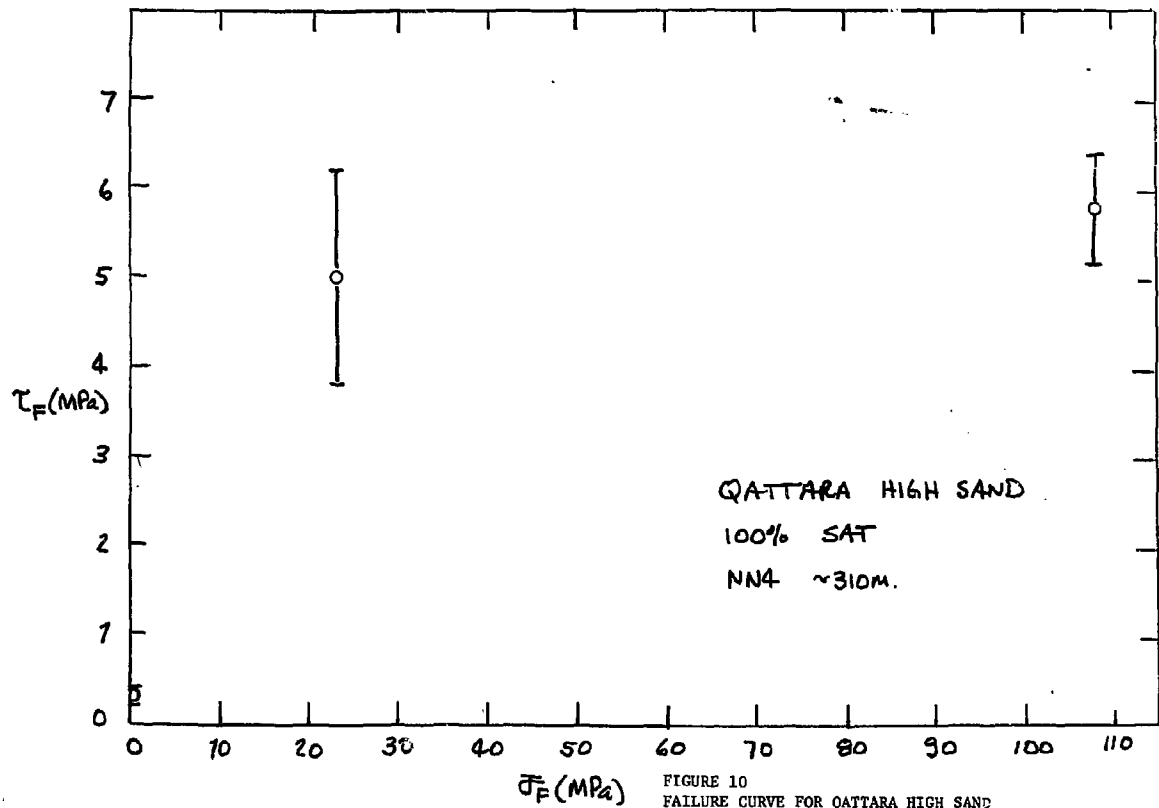


FIGURE 9  
COMPRESSIBILITY FOR QATTARA HIGH SAND



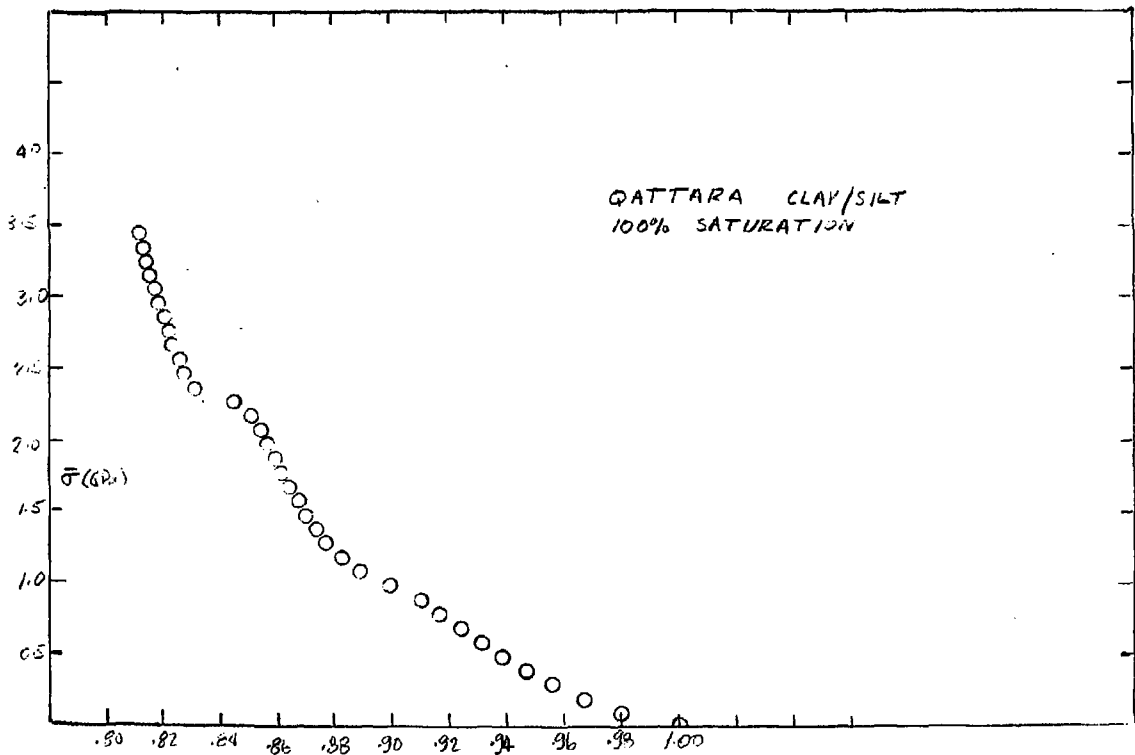


FIGURE 11  
COMPRESSIBILITY FOR QATTARA CLAY/SILT

